Chinese Chemical Letters 33 (2022) 2195–2199

Contents lists available at ScienceDirect

Chinese Chemical Letters

journal homepage: www.elsevier.com/locate/cclet

Achieving higher performances without an external curing agent in natural magnolol-based epoxy resin

Qi Cao, Zhihuan Weng*, Yu Qi, Jiahui Li, Wentao Liu, Chengde Liu, Shouhai Zhang, Zhiyong Wei, Yousi Chen, Xigao Jian

State Key Laboratory of Fine Chemicals, Liaoning High Performance Resin Engineering Research Center, Department of Polymer Science & Engineering, Dalian University of Technology, Dalian 116024, China

ARTICLE INFO

Article history:
Received 9 July 2021
Revised 14 August 2021
Accepted 6 September 2021
Available online 11 September 2021

Keywords:
Epoxy resin
Magnolol
Self-curing
Fully bio-based
Antimicrobial properties

ABSTRACT

Bio-based epoxy thermoset prepared from renewable biomass raw materials can alleviate fossil energy crisis and reduce environmental pollution, which satisfies the needs of sustainable social development. In this study, a bio-based epoxy thermoset precursor (MGOL-EP) was synthesized from a naturally occurring magnolol through a facile and efficient one-step process. And the fully bio-based epoxy thermoset (MGOL-EP-SC) was obtained by self-curing without adding any other hardener. MGOL-EP-SC revealed an extremely high glass-transition temperature (T_g) of 265 °C and char yield of 53.2% (in N_2), which were at the highest level among the fully bio-based epoxy thermosets reported so far. In addition, when the MGOL-EP was cured with 4,4′-methylenedianiline (DDM), T_g of the MGOL-EP/DDM was decreased by 61 °C and the other comprehensive performance had also been decreased, which was due to a reduction in biphenyl structure content and cross-linking density by adding the external curing agents. Moreover, the MGOL-EP-SC presented certain killing rate (48.4%) to *Staphylococcus aureus*. These findings provide a new design strategy for engineering high-performance and functional epoxy thermoset with high biomass content.

Epoxy thermosets, one of the three thermosetting polymer materials, have been widely used in a multitude of fields such as protective coatings, adhesives, constructions, high-performance composites, electrical engineering, electronic encapsulation, and so forth due to their excellent dimensional stability, thermal stability, mechanical strength, creep resistance, electrical insulation and chemical resistance [1–3]. However, approximately 90% of the epoxy production is made up of bisphenol A (BPA) produced from petroleum-derived phenol [4].

Bio-based epoxy thermosets originated from renewable resources not only reduces the consumption of petroleum resources in the plastic industry, but also depress the environmental pollution caused by petrochemical raw materials in the production process, meeting the needs of sustainable development of society [5]. In the recent decade, bio-based monomer (such as epoxidized soybean oil [6,7], eugenol [8], vanillin [9], tannin acid [10], gallic acid [11] and bio-transformed small molecule phenols [12–14]) have played a vital role in the direction of bio-based epoxy thermosets with high-performance. At present, the current relevant studies focus mainly on bio-based epoxy monomers, and then the petrochemical-based curing agents (such as *m*-xylylenediamine (MXDA), 4,4′-diaminodiphenylmethane (DDM)) are used to cross-link bio-based epoxy monomers to obtain high thermo-mechanical properties and chemical resistance [15]. On the one hand, as one of the most common curing agents for epoxy thermosets, aromatic amines are often environmentally unfriendly. For example, DDM is highly toxic and has an occupational exposure limit of only 10 ppb per 8 h workday, while even short-term skin contact can have serious effects on the human liver [16]. Moreover, petrochemical-based curing agents are used to cure the epoxy thermosets mentioned above, remarkably reducing the bio-based content of the epoxy thermosets.

As far as we know, although many kinds of bio-based epoxy thermosets have been developed [17,18], few of them were fully bio-based since it requires both the epoxy monomers and curing agents come from biomass [19–21]. As the curing agents (such as diamine and multi-phenols) also play an important role in determining the properties of cured epoxy networks [22–25], some of bio-based curing agents with aromatic structure have been prepared to achieve high performance epoxy thermosets, however,

* Corresponding author.
E-mail address: zweng@dlut.edu.cn (Z. Weng).

https://doi.org/10.1016/j.cclet.2021.09.025
1001-8417/

Scheme 1. Reaction route for the synthesis of magnolol-derived epoxy (MGOL-EP).

the preparation procedures were relatively complex [20,22,26–28]. Baca *et al*. synthesized a low-toxicity resveratrol-derived aniline as a safer alternative to MXDA. Glass transition temperature (T_g) of the networks was more than 100 °C higher than that of DGEBA/MXDA networks [23]. Nabipour *et al*. synthesized a fully bio-based epoxy thermoset (SA-GA-EP/DIFFA) through curing a bio-based epoxy monomer (SA-GA-EP) by a curing agent (DIFFA) derived from syringaldehyde and furfurylamine, respectively, and the T_g of the resultant thermoset was 204 °C [26]. Whatever, the development of fully bio-based epoxy thermosets with good comprehensive performances remains a challenge.

Magnolol, a natural product containing both phenolic and alkenyl functionalities with a high aromatic content, is extracted from the bark of magnolia officinalis, and is commonly used as herbal medicine and in cosmetics [29]. Moreover, it is of non-toxic and has the strong antibacterial effect. In addition, it has been proved that the biphenyl structure in magnolol not only can improve the thermal stability, but also form a kind of highly pyrolysis-resistant carbonaceous in the combustion process to improve the intrinsic flame retardancy of the cured epoxy thermosets [30].

In this study, we developed a facile strategy to achieve a high-performance fully bio-based epoxy thermoset without external curing agent. The allyl group of magnolol was epoxidation (MGOL-EP), and then a fully bio-based epoxy thermoset of MGOL-EP-SC was obtained through self-curing of MGOL-EP, where the phenolic group acted as active curing center. The fully bio-based MGOL-EP-SC displayed more advanced properties that were competitive with DGEBA/DDM, such as higher thermal stability, intrinsically low flammability, better mechanical properties and thermochemical properties. Moreover, the highest T_g was observed for this system among all other reported fully bio-based epoxy thermosets to the best of our knowledge, and MGOL-EP-SC showed certain antibacterial ability. The findings supply a new design strategy for preparing the fully bio-based epoxy with excellent comprehensive performance.

Magnolol-derived epoxy (MGOL-EP) was synthesized *via* a simply one-step reaction as shown in Scheme 1. The allyl groups of magnolol were epoxidized into epoxy groups at room temperature in CH_2Cl_2 using 3-chloroperoxybenzoic acid (*m*-CPBA). Compared to *O*-glycidylation reaction with epichlorohydrin (ECH) and bio-based phenols, which was strongly affected by catalyst, reaction temperature, reaction time, ratios of –OH to ECH, solvents, water, bases, *etc*., the epoxidation reaction of allyl group was much more facile and efficient without side-reactions to product epoxy monomers [11]. Moreover, there was no need to isolate magnolol and MGOL-EP using column chromatography, which will be attractive for their potential scaling-up synthesis for industrial applications. The chemical structure of MGOL-EP was confirmed by NMR as shown in Fig. S1 (Supporting information). After the reaction, the ^{1}H NMR signals of allyl double bonds (5.93 and 5.03 ppm) disappeared (Fig. S1a), whereas the new proton peaks at 3.07, 2.70 and 2.58-2.51 attributed to epoxy groups appeared in the spectrum. The ^{13}C NMR (Fig. S1b) and HRMS further confirmed MGOL-EP has been synthesized successfully.

Non-isothermal differential scanning calorimetry (DSC) was employed to examine the curing behavior of MGOL-EP. The corresponding curves of various samples with different heating rates were shown in Fig. S2 (Supporting information). Surprisingly, it can be seen that MGOL-EP without any curing agent showed a single exothermic peak, which indicated the system exhibited self-curing behavior, while there was no obvious exothermic peak on pristine DGEBA. For further verification, DDM was used to cure MGOL-EP, and it was found two obvious exothermic peaks in the DSC curve, which presented the reaction of DDM between epoxy group, and self-curing behavior, respectively. Non-isothermal DSC thermographs with various heating rates and the curing activation energy (E_a) calculated according to Kissinger's method are illustrated in Fig. S2c [31]. The average E_a for MGOL-EP-SC was calculated to be 94.8 kJ/mol, which is consistent with the activation energy range of phenolic hydroxyl curing epoxy group. In addition, MGOL-EP/DDM presented lower E_a (77.0 kJ/mol), which may be due to the presence of the tertiary amine functional group, and the tertiary amine structure could also promote the curing of the MGOL-EP/DDM system.

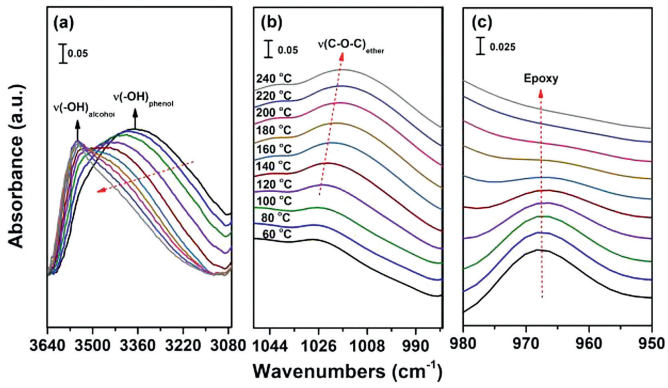

Fig. 1. The *in-situ* FTIR of the MGOL-EP monomer heated from 60 °C to 240 °C scanned with a 20 °C interval. (a) The stretching vibration of –OH; (b) the stretching vibration of –C–O–C–; (c) the stretching vibration of epoxy groups.

Furthermore, the self-curing reaction of MGOL-EP was monitored through *in-situ* infrared in the temperature range of 60-240 °C [32]. As shown in Fig. 1, the bands in the spectrum of MGOL-EP at 965 and 3350 cm^{-1} were ascribed to the epoxy and phenolic hydroxyl groups, respectively. Within the tested temperature range, when the temperature exceeded 120 °C, the curing reaction started, and the characteristic absorption peak of MGOL-EP began to change obviously, which was consistent with the result that it began to exothermic around 120 °C in the DSC curve. According to the previous reports, if a certain group participated in the formation of hydrogen bonds, it will lead to longer intermolecular or intramolecular bond length, lower bond energy and *k* value [33]. As a result, the absorption frequency moved towards the lower wavenumber. As can be seen from Fig. 1a, the stretching vibration peak of –OH moved from 3350 cm^{-1} to a higher wavenumber of 3549 cm^{-1}, which indicated that the hydrogen bond gradually dissociated during the heating process. In addition, when the temperature was incresed from 120 °C to 240 °C, this broad band decreased and a new -OH peak (3549 cm^{-1}) occurred attributed to the generation of hydroxyl groups by the ring-opening reaction of epoxy group [34]. And this also was confirmed by the decreasing absorption peak of epoxy groups at 965 cm^{-1} as shown in Fig. 1c. In the meantime, the position around 1016 cm^{-1} appeared new stretching vibration peak, which was attributed to the ether bond (C–O–C) formed by the reaction of phenolic hydroxyl group and epoxy [28].

Based on the above discussion, the proposed self-curing mechanism of MGOL-EP can be illustrated in Scheme 2. Firstly, the epoxy groups and the phenolic hydroxyl groups formed hydrogen bonds,

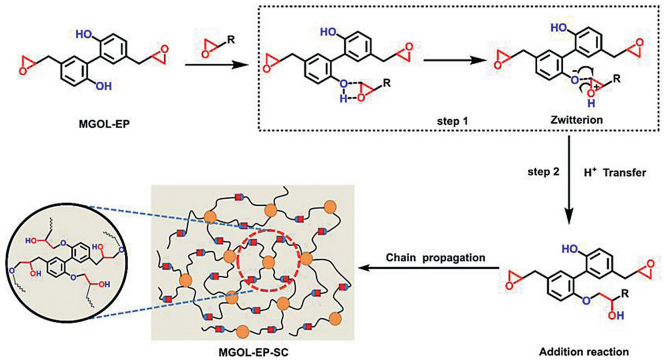

Scheme 2. Self-curing behavior and the proposed self-curing mechanism of MGOL-EP.

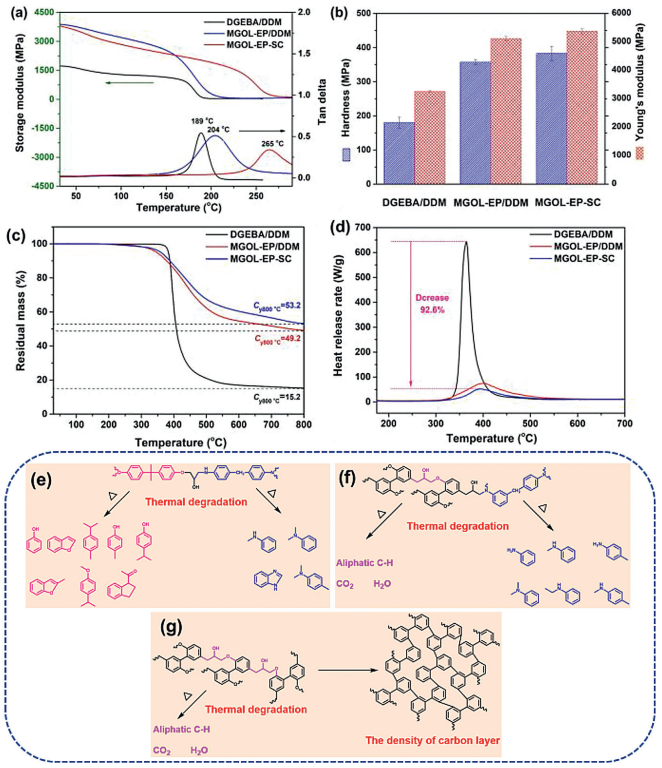

Fig. 2. (a) DMA spectra for storage modulus and tanδ against temperature of DGEBA/DDM, MGOL-EP/DDM and MGOL-EP-SC. (b) The hardness and Young's modulus of DGEBA/DDM, MGOL-EP/DDM and MGOL-EP-SC obtained from nanoindentation.(c) TGA curves of the cured DGEBA/DDM, MGOL-EP/DDM and MGOL-EP-SC with heating rate of 20 K/min under N_2 atmosphere. (d) Heat release rate *versus* temperature curves from MCC tests for DGEBA/DDM, MGOL-EP/DDM and MGOL-EP-SC. Proposed pyrolysis routes for (e) DGEBA/DDM, (f) MGOL-EP/DDM, (g) MGOL-EP-SC.

and then the oxygen atom of the epoxy groups turned to be a transition state of oxonium salt in step 1. The unstable oxonium salt can easily be cyclized to produce stable carbocation, and then the oxygen negative ion of phenolic hydroxyl can combine with the intermediate carbocation to complete the addition reaction in step 2. The addition reaction of MGOL-EP kept going on and gradually led to a network.

The thermomechanical performances of cured epoxy thermosets were investigated by dynamic mechanical analysis (DMA). The temperature effects on the storage modulus (E') and tanδ of DGEBA/DDM, MGOL-EP/DDM and MGOL-EP-SC were shown in Fig. 2a, and the corresponding parameters were collected in Table S1 (Supporting information). MGOL-EP systems showed higher E' compared with DGEBA/DDM during the entire experimental temperature range. Particularly at 32 °C, the E' of MGOL-EP/DDM and MGOL-EP-SC reached 3884 MPa and 3789 MPa, which were 125.9% and 119.4% higher than that of DGEBA/DDM (1727 MPa), respectively. Moreover, MGOL-EP-SC achieved a T_g of 265 °C, which was much higher than those of MGOL-EP/DDM (204 °C) and DGEBA/DDM (189 °C). Generally, T_g is influenced primarily by the cross-link density, the rigidity of chain segments and interaction between thermoset segments [35,36]. The crosslink density V_e of the thermosets can be calculated from the eq. S3 obtained from the rubber elasticity theory [35].

In Table S1, The V_e of MGOL-EP-SC was calculated to be 8713 mol/m^3, which was much higher than those of MGOL-EP/DDM (4634 mol/m^3) and DGEBA/DDM (3048 mol/m^3). As illustrated in Scheme 2, it can be found that the MGOL-EP did not have any redundant substituents (such as methoxy substituents [37]) and could be as special tetra-functional epoxy precursor during the self-curing progress, which led to higher V_e in the MGOL-EP-SC system. However, when the MGOL-EP was cured with DDM, T_g of the MGOL-EP/DDM was decreased by 61 °C, which was due to a reduction in biphenyl structure content and cross-linking density by adding the external curing agents. Therefore, the high T_g of MGOL-EP-SC was attributed to the rigid biphenyl moiety and high cross-linked density after self-curing reaction.

Nanoindentation is a simple and effective method to measure the mechanical properties of material with very small samples, it also has been successfully used to measure the mechanical properties of the cured epoxy [38,39]. As shown in Fig. 2b and Table S1, the Young's modulus and hardness of MGOL-EP-SC were 5372 MPa and 383 MPa, respectively, which were 64.8% and 112.8% higher than those of DGEBA/DDM, respectively. The excellent mechanical properties of MGOL-EP-SC were attributed to the introduction of the rigid biphenyl moiety in MGOL-EP molecule and high cross-linked density formed in the network. Based on the high T_g and excellent mechanical properties of MGOL-EP-SC, it has great potential in replacement of petroleum-based resins for application in aerospace industrial, electrical engineering, electronic encapsulation and so on.

The thermal stability of the cured epoxy samples was studied by thermogravimetric analysis (TGA) under N_2, and it was often indicated by the statistic heat-resistant index (T_s) calculated with degradation temperature of 5% weight loss ($T_{d5\%}$) and degradation temperature of 30% weight loss ($T_{d30\%}$) [19], the detailed data was summarized in Fig. 2c and Table S2 (Supporting information). The MGOL-EP-SC exhibited higher T_s (213 °C) than DGEBA/DDM (192 °C) and MGOL-EP/DDM (204 °C). In spite of that, the initial decomposition temperature of MGOI-EP-SC was still significantly higher than its T_g, showing satisfactory thermal stability for practical applications. More impressively, the char yield of MGOL-EP-SC reached 53.2% at 800 °C, showing 2.5-fold that of DGEBA/DDM (15.2%). Usually, the char formation will insulate the polymer-air interface, reduce the heat conduction, and starve the combustion process of decomposition products [5]. This result indicated that MGOL-EP-SC should have good intrinsic flame retardation. As depicted in Fig. S3 (Supporting information), the maximum degradation rate (R_{max}) of MGOL-EP-SC (0.225%/min) was far lower than that of DGEBA/DDM (2.417%/min) and the reduction was 90.7%, indicating that the MGOL-EP-SC possesses an excellent inhibition effect over thermal degradation.

Microscale combustion calorimetry (MCC) and the limiting oxygen index (LOI) are rapid effective method for assessing the flammability of the cured epoxy thermosets [29]. The heat release rate (HRR) against temperature curves of cured epoxy thermosets was shown in Fig. 2d, and the corresponding data (the total heat release (THR), the peak heat release rate (PHRR) and the peak heat release temperature (T_{peak})) are displayed in Table S3 (Supporting

information). The HRR value is an important parameter that can be served as the main indicator of the fire-safety properties of materials [40]. Noteworthy, the PHRR of DGEBA/DDM was up to 636.3 W/g, whereas MGOL-EP-SC and MGOL-EP/DDM exhibited the PHRR values of 47.12 and 67.08 W/g, the reduction was about 92.6% and 89.5%, respectively. Moreover, the reduction in THR for MGOL-EP-SC and MGOL-EP/DDM was up to 70.6% and 54.3%, respectively, compared with that of DGEBA/DDM (5.8 kJ/g *vs*. 19.7 kJ/g; 9 kJ/g *vs*. 19.7 kJ/g). The results showed that MGOL-EP-SC had a LOI of 38.8%, which was higher than those of DGEBA/DDM (23.6%) and MGOL-EP/DDM (37.2%), confirming its high flame-retardant potential. According to the literature, the materials with LOI above 28% are considered as "self-extinguishing" materials [41]. The MCC and TGA results support the low flammability of MGOL-EP-SC, which is associated with the special tetra-functional structure including highly aromatic biphenyl. After self-curing progress, such highly compact aromatic rings will reduce the production of gaseous combustible by promoting charring. In short, MGOL-EP-SC endows the cured epoxy with the low flammability, hence improving the fire safety.

In order to investigate the thermal degradation mechanism, TG-IR-GC/MS was used to monitor the pyrolysis components during thermal degradation process [42]. Fig. S4a (Supporting information) shows the FTIR spectra of pyrolysis gaseous products of DGEBA/DDM, MGOLEP/DDM and MGOL-EP-SC at the temperature of maximum degradation rate (395, 439 and 437 °C, respectively). The main gas products of DGEBA/DDM, MGOL-EP/DDM and MGOL-EP-SC were identified by the characteristic bands of water and/or phenol (3649 cm^{-1}), various hydrocarbons (3185–2800 cm^{-1}), CO_2 (2400–2250 cm^{-1}, 670 cm^{-1}), CO (2200–2045 cm^{-1}), carbonyl compounds (1762 cm^{-1}), aromatic compounds (1610 cm^{-1}, 1510 cm^{-1}), Ar-N (1326 cm^{-1}), Ar-O (1260 cm^{-1}) and aliphatic ethers (1177 cm^{-1}) [5,35]. Because the same weight was taken in tests, the intensity of absorption peak can intuitively reflect the amount of degradation products. In comparison, the intensities of absorption peaks of MGOL-EP-SC were much lower than those of DGEBA/DDM and MGOL-EP/DDM, which indicated that MGOL-EP-SC released much less pyrolysis products at the temperature of maximum degradation rate. In addition, the absorbance intensities of aromatic compounds, carbonyl compounds, aliphatic C–H compounds, CH_4 during the whole thermal degradation process are presented in Figs. S4b-f (Supporting information). It is worth noting that the DGEBA/DDM system produced large numbers of phenol, aromatic compounds, Ar-N, Ar-O and aliphatic ethers, which demonstrated that the backbone of DGEBA/DDM system was broken down. Whereas only trace aromatic products were detected in the MGOL-EP systems, which indicated that most of the aromatic structures still remained in the backbone of resulting resins and formed stable rich aromatic char layer to further enhance the flame retardancy.

To understand the thermal degradation mechanism and its contribution to the flame retardancy of the MGOL-EP-SC system, the TG-GC/MS test was performed, which the cracker temperature was set at 400 °C and the resulting gas is pumped into GC/MS. [36] Fig. S5 (Supporting information) shows the total ion chromatograms of DGEBA/DDM, MGOL-EP-SC and MGOL-EP/DMM, and the structures of pyrolytic products are listed in Table S5 (Supporting information). In case of the DGEBA/DDM, the major pyrolysis components were numerous aromatic compounds, such as phenol (peak 1), benzofuran (peak 2), *p*-cymene- (peak 3), *p*-cresol (peak 4), 4-isopropylphenol (peak 5), 2-methylbenzofuran (peak 9), 1-isopropyl-4-methoxybenzene (peak 10) and 1-(2,3-dihydro-1H-inden-1-yl) ethan-1-one (peak 12). All these pyrolysis components were produced from the bisphenol A fragments of DGEBA/DDM. Other products (such as *N*-methylaniline (peak 6), *N*,*N*-dimethylaniline (peak 7), 1*H*-benzo[*d*]imidazole (peak 8) and *N*,4-dimethylaniline (peak 11)) were produced during the pyrolysis process of the 4,4′-methylenedianiline fragments. On the basis of these observations, the pyrolysis route for DGEBA/DDM has been presented in Fig. 2e. In the pyrolysis process of MGOL-EP/DDM system, some aromatic components included aniline (peak b), *N*-methylaniline (peak c), *p*-toluidine (peak d), *N*,*N*-dimethylaniline (peak e), *N*-ethylaniline (peak f) and *N*,4-dimethylaniline (peak h) were also released, which indicated that 4,4'-methylenedianiline segments were cleaved from the main chain of MGOL-EP/DDM, and the biphenyl structures remained intact. The thermal degradation mechanism of MGOL-EP/DDM system has been depicted in Fig. 2f. According to the thermal degradation mechanism of MGOL-EP/DDM, it found that the higher biphenyl structure content is beneficial to improve the thermal stability of the system. Compared to the MGOL-EP/DDM system, the MGOL-EP-SC system can not only increase the content of biphenyl structure, but also increase the cross-linking density of the system by self-curing reaction. The total ion chromatograms of TG-GC/MS for MGOL-EP-SC hardly found any peak, it was concluded that MGOL-EP-SC released fewer volatile products during the pyrolysis process and more aromatic components were remained in the condensed phase, which led to its high char yield. Based on above results and analysis, thermal degradation mechanism of MGOL-EP-SC is proposed in Fig. 2g. When the temperature was increased, the Ar-C and Ar-O bonds were cleaved, which led to the formation the biphenyl radical intermediates. Subsequently, the biphenyl radical intermediates were randomly combined to form a stable aromatic/graphite char layer by crosslinking, arrangement and dehydrogenation [30]. The rich char layer effectively blocked the transfer of the heat and flammable gas transfer, and protected the internal resin matrix from further degradation. Meanwhile, CO_2 and H_2O were found during the thermal degradation process, the nonflammable CO_2 and H_2O could take away the heat and diluted the concentration of oxygen and other flammable gases, which enhanced the flame retardancy of this system. This thermal degradation mechanism is consistent with the TGA and MCC results.

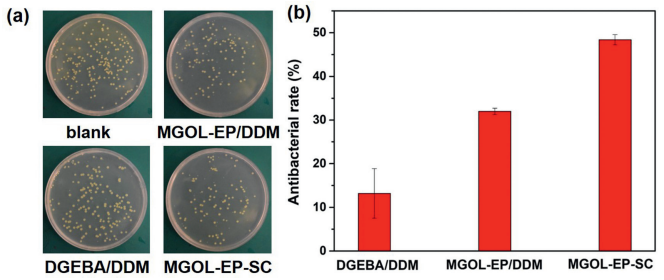

Fig. 3. (a) Digital photos of *Staphylococcus aureus* colonies survived on the nutrient agar plates after treatment with blank, DGEBA/DDM, MGOL-EP/DDM and MGOL-EP-SC. (b) The antibacterial rates against *Staphylococcus aureus* of various samples.

In view of the good antibacterial property of magnolol, it was expected that the prepared magnolol-based thermosets could also show similar properties in this work. The antibacterial activities of the DGEBA/DDM, MGOL-EP/DDM and MGOL-EP-SC against *Staphylococcus aureus* (*SA*, Gram-positive bacteria) were investigated by the plate count method. Digital photos of the antibacterial effects and the antibacterial rates of the resulting thermosets against *SA* were illustrated in Figs. 3a and b. It was clear that MGOL-EP-SC and MGOL-EP/DDM had certain antibacterial ability, and the antibacterial rates against *SA* were 48.40% and 31.98%, respectively, which was 3.7 and 2.4-fold higher than that of DGEBA/DDM. This was due to the MGOL-EP-SC resins can damage the cell surface, resulting in increased membrane permeability, leakage of cell components and inhibition of SA growth [43,44]. These results indicated that the high performance fully bio-based thermoset should

be a promising candidate for antibacterial coatings, antibacterial bio-medical devices and other antibacterial materials.

In this study, a facile and sustainable route was supplied to prepare a magnolol-derived compound (MGOL-EP), which could be used as both multifunctional hardener and epoxy precursor. After self-curing reaction, MGOL-EP-SC revealed an extremely high glass-transition temperature of 265 °C and char yield of 53.2% (in N_2), which were at the highest level among the fully bio-based epoxy thermosets reported so far. In comparison with DGEBA/DDM, MGOL-EP-SC expressed significantly improved mechanical properties (64.8% and 112.8% enhancement in Young's modulus and hardness, respectively), intrinsically low flammability and high thermal stability. The introduction of magnolol structure made the MGOL-EP-SC have certain antibacterial ability. Besides, it is interesting that the self-cured epoxy thermoset, MGOL-EP-SC, showed better comprehensive properties than MGOL-EP/DDM cured with external curing agent DDM. Thus, due to these attractive properties, MGOL-EP-SC holds a great potential as the composite resin matrix to satisfy more demanding and even in cutting-edge applications.

Declaration of competing interest

The authors declare that they have no known competing financial interests or personal relationships that could have appeared to influence the work reported in this paper.

Acknowledgments

This work was supported by the National Natural Science Foundation of China (Nos. 51873027, 52073038 and 51673033), the Natural Science Foundation of Liaoning Province (No. 2019-ZD-0139), the Fundamental Research Funds for the Central Universities (No. DUT20TD114) and the National Key Research and Development Program of China (No. 2017YFB0307600).

Supplementary materials

Supplementary material associated with this article can be found, in the online version, at doi:10.1016/j.cclet.2021.09.025.

References

[1] J.X. Wang, K.T. Chen, S.T. Huang, C.C. Chen, Chin. Chem. Lett. 22 (2011) 1363–1366.
[2] C. Gioia, G. Lo Re, M. Lawoko, L Berglund, J. Am. Chem. Soc. 11 (2018) 4054–4061.
[3] Z. Xu, Y. Liang, X. Ma, et al., Nature Sustain. 1 (2019) 29–34.
[4] J. Cheng, J. Chen, W.T. Yang, Chin. Chem. Lett. 18 (2007) 469–472.
[5] Y. Qi, Z. Weng, Y. Kou, et al., Compos. Part B: Eng. 214 (2021) 108749–108759.
[6] Y.F. Lei, X.L. Wang, B.W. Liu, L. Chen, Y.Z. Wang, Chin. Chem. Lett. 32 (2021) 875–879.
[7] L.J. Sun, C. Yao, H.F. Zheng, J. Lin, Chin. Chem. Lett. 23 (2012) 919–922.
[8] T. Liu, C. Hao, S. Zhang, et al., Macromolecules 51 (2018) 5577–5585.
[9] W. Yuan, S. Ma, S. Wang, et al., Eur. Poly. J. 117 (2019) 200–207.
[10] X. Feng, J. Fan, A. Li, G. Li, ACS Sustain. Chem. Eng. 8 (2019) 874–883.
[11] Y. Tao, L. Fang, M. Dai, et al., Polym. Chem. 11 (2020) 4500–4506.
[12] Y. Qi, J. Wang, Y. Kou, et al., Nat Commun 10 (2019) 2107–2116.
[13] X. Wang, W. Guo, L. Song, Y. Hu, Compos. Part B: Eng. 179 (2019) 107487–107500.
[14] Y. Jiang, D. Ding, S. Zhao, et al., Green Chem. 20 (2018) 1131–1138.
[15] X. Xu, S. Ma, J. Wu, et al., J. Mater. Chem. A 7 (2019) 15420–15431.
[16] B.G. Harvey, G.R. Yandek, J.T. Lamb, et al., RSC Adv. 7 (2017) 23149–23156.
[17] J. Wan, J. Zhao, X. Zhang, et al., Pro. Polym. Sci. 108 (2020) 101287–101332.
[18] Z. Fang, S. Nikafshar, E.L. Hegg, M. Nejad, ACS Sustain. Chem. Eng. 8 (2020) 9095–9103.
[19] C.H. Chen, C.M. Lin, T.Y. Juang, M.M. Abu-Omar, C.H. Lin, Polym. Chem. 10 (2019) 3983–3995.
[20] X. Yang, L. Guo, X. Xu, S. Shang, H. Liu, Mater. Des. 186 (2020) 108248–108258.
[21] X. Chen, S. Chen, Z. Xu, J. Zhang, M. Miao, Zhang D, Green Chem. 22 (2020) 4187–4198.
[22] H. Memon, H. Liu, M.A. Rashid, et al., Macromolecules 53 (2020) 621–630.
[23] M.D. Garrison, M.A. Savolainen, A.P. Chafin, et al., ACS Sustain. Chem. Eng. 8 (2020) 14137–14149.
[24] S. Zhang, T. Liu, C. Hao, et al., Green Chem. 20 (2018) 2995–3000.
[25] H. Wang, B. Liu, X. Liu, J. Zhang, M. Xian, Green Chem. 10 (2008) 1190–1196.
[26] H. Nabipour, X. Wang, L. Song, Y. Hu, Green Chem. 23 (2021) 501–530.
[27] Z. Weng, Y. Qi, K. Zhang, et al., Chin. J. Bioprocess Eng. 17 (2019) 437–442.
[28] M. Qi, Y. Xu, W. Rao, et al., RSC Adv. 47 (2018) 26948–26958.
[29] K.T. Wacker, A.C. Weems, S.M. Lim, et al., Biomacromolecules 20 (2019) 109–117.
[30] Y. Qi, Z. Weng, K. Zhang, et al., Chem. Eng. J. 387 (2020) 124115–124129.
[31] N.G. Jaques, J. William de Lima Souza, M. Popp, et al., Compos. Part B: Eng. 183 (2020) 107651–107665.
[32] W. Peng, F. Yao, J. Hu, et al., Green Chem. 20 (2018) 5158–5168.
[33] J. Hu, Z. Wang, Z. Lu, et al., Polymer 119 (2017) 59–65.
[34] X. Fei, W. Wei, F. Zhao, et al., ACS Sustain. Chem. Eng. 5 (2016) 596–603.
[35] Y. Qi, Z. Weng, Y. Kou, et al., Chem. Eng. J. 406 (2021) 126881–126893.
[36] J. Shen, X Lin, J. Liu, X. Li, Macromolecules 52 (2018) 121–134.
[37] S. Zhao, X. Huang, A.J. Whelton, M.M. Abu-Omar, ACS Sustain. Chem. Eng. 6 (2018) 7600–7608.
[38] J. Wan, B. Gan, C. Li, et al., Chem. Eng. J. 284 (2016) 1080–1093.
[39] Y. Li, O. Rios, M.R. Kessler, ACS Appl. Mater. Inter. 6 (2014) 19456–19464.
[40] J. Dai, Y. Peng, N. Teng, et al., ACS Sustain. Chem. Eng. 6 (2018) 7589–7599.
[41] T. Weiss, H. Schuster, J. Muller, et al., Ann. Occup. Hyg. 55 (2011) 886–892.
[42] P. Gnanasekar, H. Chen, N. Tratnik, M. Feng, N. Yan, Compos. Part B: Eng. 207 (2021) 108585–108597.
[43] E.J. Choi, H.I. Kim, J.A. Kim, et al., Appl. Microbiol. Biotechnol. 99 (2015) 4387–4396.
[44] C.F. Lin, C.F. Hung, I.A. Aljuffali, et al., Pharm. Res. 33 (2016) 1–16.